Influence of Patient Size and Photon Energies on IMRT Plans for Localized Prostate Cancer

Khabat A. Mohammed[1†] and Kharman A. Faraj[2]

[1]Department of Physics, College of Education, University of Sulaimani, Sulaymaniyah 41005, Kurdistan Region – F.R. Iraq

[2]Department of Physics, College of Science, University of Sulaimani, Sulaymaniyah 41005, Kurdistan Region – F.R. Iraq

***Abstract*—The localized prostate cancer treatment with intensity-modulated radiation therapy (IMRT) produces precise radiation doses that protect healthy tissues but continues to generate toxicity in the bladder and rectum. Our study aims to evaluate how patient size and photon energy influence IMRT plan quality in localized prostate cancer. Patients with localized prostate cancer (n = 20) received IMRT treatment in a retrospective analysis through two groups (small n = 12 and large n = 8) based on planning target volume isocenter diameter measurements. The same planning objectives guided the build of 6 MV and 10 MV photon plans for each patient. The assessment included monitor units (MUs) as well as examination of homogeneity index and conformity index, and dose–volume histogram metrics when comparing different energies and patient size groups. The target coverage and dose uniformity between 6 MV and 10 MV were equivalent, but 10 MV plans cut down MUs by 6.6% in a small group. The size of patients played a stronger influence on organs at risk (OAR) than energy utilization during treatment planning. Large patients received 22% lower mean bladder doses, 30% lower bladder V10–V50 values, and 33–96% (6 MV) less V20–V50 doses in the left femoral head compared to smaller patients. The size of the patient influenced OAR sparing more than the selection of photon energy, which had limited and size-dependent effects. Therefore, patient size has to be considered in energy choice, treatment planning, and clinical trial design to individualize treatment and minimize toxicity.**

***Index Terms*—Dosimetric analysis, Intensity-modulated radiation therapy, Patient size, Photon energy, Prostate cancer, Radiotherapy planning.**

I. Introduction

Prostate cancer exists as a frequently occurring cancer that stands as one of the principal contributors to male cancer fatalities (Bergengren, et al., 2023; Schafer, et al., 2025). The treatment approach for each patient depends on their age and disease stage in combination with their overall health status. Radical prostatectomy or radiation therapy is standard treatment choices for patients with localized disease, which represents about 75% of cases (Evans, 2018; Raychaudhuri, Lin and Montgomery, 2025). People with advanced disease must receive systemic therapy options (Teo, Rathkopf and Kantoff, 2019). Radiotherapy has a curative intent and its use is well established, even in intermediate risk or cases with minor nodal involvement, and in advanced stages it is palliative (relieves symptoms, improves quality of life) (Hatano, et al., 2019).

Most recently, intensity-modulated radiation therapy (IMRT) has transformed dose shaping in external-beam radiotherapy (Webb, 2003). IMRT splits beams into hundreds or thousands of "beamlets" with each beamlet having its own intensity that is optimized using inverse-planning algorithms. Using the concept of modulating these beamlets at different angles, IMRT is able to produce very conformed dose distributions with concave isodose lines that closely envelope irregular tumor volumes without hitting adjacent organs at risk (OAR) (Mukherjee, Small and Duszak, 2022). Thereby, IMRT has ended up as one of the most prevalent and successful methods of treating prostate cancer (Agrawal, et al., 2022).

The use of IMRT provides significant advantages in cancer therapy, but radiation side effects to critical organs, such as the bladder and rectum present a risk of developing secondary tumors (Lin, et al., 2023). These issues indicate the necessity of an even greater reduction of radiation toxicity in prostate IMRT. The characteristics of the photon beam and individual patient anatomical dimensions determine how the radiation dose is distributed throughout the treatment area, and, as a result, may impact dose distribution to those critical organs.

A publication has compared 6 MV photon with other energies (10 MV, 15 MV, or 18 MV) and yielded conflicting results in monitor-unit reduction and modest preservation of normal tissue. For localized prostate cancer, earlier work by De Boer, et al., in 2007 (10 patients, 5 beams) compared 6 MV and 18 MV plans and reported a non-major difference in target coverage or organ-at-risk doses. Thangavelu et al., in 201 (8 patients, 5 beams) compared 6 MV versus 15 MV beams and noted slightly improved conformity, homogeneity, and

ARO-The Scientific Journal of Koya University
Vol. XIII, No.2(2025), Article ID: ARO.12243. 8 pages
DOI: 10.14500/aro.12243
Received: 30 April 2025; Accepted: 03 August 2025
Regular research paper; Published: 23 September 2025
†Corresponding author's e-mail: xabat.muhammad@univsul.edu.iq

2–4% lower rectal volumes receiving high dose with 15 MV. Chung, et al., 2011 (10 patients, 7 beams) compared 6 MV versus 15 MV and reported that the 6 MV plans required 13.4% more monitor units (MUs) than the 15 MV plans, whereas the 15 MV plans yielded marginally better dose distributions to the rectum, bladder, and femoral heads. Solaiappan, et al., 2009 (20 patients, 5 beams) compared 6 MV and 10 MV beams. Contrary to previous studies, they found that the 10 MV plans delivered higher doses to 15% volume of the bladder and rectum. None of the above studies on localized prostate cancer reported p-values. Sung, et al., 2012 (20 patients, 8 beams) performed statistical analyses on prostate cancer cases involving seminal vesicles using 6 MV, 10 MV, and 15 MV beams. They achieved similar target coverage, conformity, and homogeneity across energies, but higher doses to the rectal wall and femoral heads with 6 MV than with the higher energies ($p < 0.05$). Those studies were done at prescription doses of 70–81 Gy in 2 Gy fractions. None of them have assessed photon-energy effects with the moderate hypofractionation schedule of 60 Gy in 3 Gy fractions (Dearnaley, et al., 2016; Morgan, et al., 2018; Pryor, et al., 2018; Mottet, et al., 2021). In addition, all these studies did not investigate the interaction of photon energy with patient size, nor did they study the independent effect of the anatomy on the dose distribution.

The effect of patient size is not commonly considered in IMRT. The only study by Stanley, et al., 2015 demonstrated how individual anatomical patient factors influence volumetric modulated arc therapy (VMAT) dose distribution patterns in prostate cancer involving lymph nodes; however, their research does not directly apply to IMRT. On the other hand, breast size has become more consistently addressed in both radiotherapy plan (Bhatnagar, et al., 2006) and in the analysis of clinical breast cancer studies (Ratosa, Jenko and Oblak, 2018). In general, increasing breast size increases dose and radiation toxicity in normal tissues.

One should also take into account neutron production in the case of higher photon energies. Kry, et al., in 2005 demonstrated that significant neutrons are generated by 15 MV and 18 MV beams; none are produced at 6 MV, and only a few at 10 MV. These neutrons also leak and can cause more danger of secondary malignancies. Hence, photon energies beyond 10MV are not preferably used in IMRT (Followill, Nüsslin and Orton, 2007).

This research addresses the information gap through a comprehensive evaluation of 6 MV and 10 MV beam dosimetry effects in prostate IMRT radiotherapy with explicit patient size considerations. The evaluation of MUs and dose homogeneity and conformity with mean dose and dose–volume histograms (DVHs) parameters enables optimization of treatment planning and toxicity reduction for personalized radiotherapy of localized prostate cancer.

II. Materials and Methods

A. Patient Selection

We conducted a retrospective review of 20 localized prostate cancer patients who were treated with IMRT at Zhianawa Cancer Center in Sulaimani, Iraq. All patients had clinical stages ranging from T1 to T2. The mean patient age was 71.6 years (range 53–83 years). Each patient had a single planning target volume (PTV) that ranged from 73 to 218 cm^3 (mean: 136 cm^3). Anatomical measurements, determined on transverse computed tomography (CT) slices at the PTV isocenter, varied from 24.34 to 30.92 cm (mean: 27.55 cm). The patient size was calculated using (1) according to Boone, et al., in 2011; Stanley, et al., in 2015:

$$Patient\ size = \sqrt{APD \times LRD} \quad (1)$$

In this formula, APD represents the anterior-posterior dimension and LRD the left-right dimension, both measured in centimeters (Fig. 1). Based on these values, patients with sizes below 27.55 cm were assigned to the small group (n = 12), and those above to the large group (n = 8). The mean values in the small and large groups were 26.3 cm and 29.4 cm, respectively.

B. Treatment Planning

All patients underwent IMRT delivered initially with 6 MV photon beams. For each case, treatment plans were developed for both 6 MV and 10 MV photon energies using identical simulation parameters set by a dedicated medical physicist. CT scans were acquired by the center's physics team, and the PTV, along with OARs – including the bladder, rectum, penile bulb (PB), and both right and left femoral heads (RT-FH and LT-FH) – were contoured by the oncology team. The planning process utilized Elekta Monaco version 5.51.10 and adhered to the center's standardized protocols for IMRT. Elekta Monaco is a commercial radiotherapy treatment-planning system using a Monte Carlo approach-based dose-calculation engine and inverse-planning to optimize IMRT and VMAT plans. It provides high-resolution photon beam delivery (multileaf collimator motion) modeling, allows complex beam geometry, contouring, dose volume analysis, and plan evaluation with user-controllable statistical uncertainty settings.

The treatment was prescribed at the isocenter, delivering a total dose of 60.0 Gy in 20 fractions (3 Gy per fraction) (Dearnaley, et al., 2016; Pryor, et al., 2018). Plans were optimized to ensure that at least 95% of the PTV received the prescribed dose while restricting the maximum dose to under

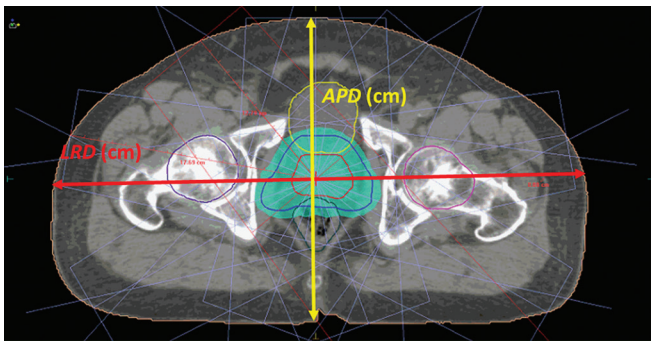

Fig. 1. Transverse computed tomography slice through the planning target volume isocenter illustrating the anterior-posterior (yellow arrow) and left-right (red arrow) dimensions used to calculate patient size.

110% of the prescription. A nine-field beam arrangement was employed with fixed gantry angles (0°, 40°, 80°, 120°, 160°, 200°, 240°, 280°, and 320°) (Pirzkall, et al., 2002); both the collimator and couch were set to 0°. The ELEKTA MLCi2 system produced beam shapes, while X-ray Voxel Monte Carlo (XVMC version 1.6) (Sethi, et al., 2013) generated dose calculations keeping statistical uncertainty at 1.00% per calculation. Treatments were delivered through the Step and Shoot IMRT technique. Specific normal tissue constraints are listed in Table I. The medical physics and oncology staff members thoroughly reviewed all plans for final approval.

C. Comparative Evaluation

Dosimetric analysis focused on comparing 6 MV and 10 MV plans as well as the impact of patient size. Cumulative DVH curves were generated by binning the dose to each voxel in 1 cGy increments from 0 Gy to the prescription dose. A statistical analysis of DVHs was performed for small and large patient populations, while specific dose–volume metrics (V10, V20, V30, V40) received detailed examination. Planning metrics such as MUs were assessed during evaluation. The Homogeneity Index (HI) served to measure dose homogeneity inside the PTV by calculating HI from (2) (ICRU, 2010):

$$HI = \frac{D_{2\%} - D_{98\%}}{D_{50\%}} \quad (2)$$

Where $D_{2\%}$, $D_{50\%}$ and $D_{95\%}$ are the doses received by 2%, 50%, and 98% of the PTV, respectively, a value near zero indicates high uniformity. The Conformity Index measurement calculates the volume relationship between tissue areas receiving at least 95% of the prescribed dose compared to the PTV volume, where 1 indicates perfect conformity (Zhai, et al., 2013).

Finally, the mean dose in the PTV and OARs was taken into consideration and is directly computed by software based on the differential DVH using (3):

$$Mean\,Dose = \frac{\sum_i D_i \Delta V_i}{\sum_i \Delta V_i} \quad (3)$$

D_i is the midpoint dose of bin i and ΔV_i is the absolute volume in that bin.

D. Statistical Analyses

The inferential statistics in R (RStudio v3) (TEAM, 2009) were used to analyze all dosimetric and plan quality metrics. The comparison of photon-energy schemes (6 MV vs. 10 MV) in the same patient was carried out by paired t-tests to address the repetition effect. To compare the impact of the patient size (small and large) of each energy scheme, Welch's t-test was applied, which can handle unequal variances of the various groups. A statistical significance level of $p < 0.05$ was used for all tests. Dosimetric data were exported directly from Elekta Monaco v5.51.10 as raw outputs and imported into R without any additional transformation; only the patient-size measurements were manually extracted from CT images. All the scripts used in the analysis and raw data are retained to ensure complete reproducibility of results.

TABLE I
Dose Constraints for Normal Tissue Tolerance (Pryor, et al., 2018)

Organ	Dose Constraint Details
Bladder	V60 ≤ 5%, V50 ≤ 30% and V40 ≤ 50%
Rectum	V57 ≤ 15% and V30 ≤ 50%
Penile Bulb	Mean dose ≤ 25–35 Gy
Femoral Head	V35 < 5%

III. Results

A. MUs

Table II shows that small patients needed 6.6% less MUs for 10 MV plans (907 ± 165) compared to 6 MV plans (971 ± 178; p = 0.035). When analyzing large patients, the trends matched but failed to achieve statistical significance (p = 0.141). Each beam energy required relatively similar MU between small patient groups and large patient groups.

B. Target Conformity and Homogeneity

The results from Table III indicate that both energies led to similar levels of target coverage and kept dosimetric homogeneity at equal levels. In small patients, the HI was 0.141 ± 0.051 for 6 MV and 0.133 ± 0.054 for 10 MV (a 5.7% reduction), with CI values nearly identical (0.972 vs. 0.975). Large patients exhibited similar trends with minimal differences. Comparisons between small and large patients yielded minimal differences, with p-values of 0.798 and 0.921 for HI, and 0.672 for CI in both photon energies.

C. Target and Normal Tissue Mean Dose Comparison

Table IV indicates that for 6 MV plans, large patients had approximately 21% lower bladder doses compared to small patients (17.62 Gy vs. 22.38 Gy; p = 0.0024). In addition, the rectum doses in large patients were about 2% lower, the PB doses around 6.6% higher, the RT-FH doses roughly 10% lower, and the LT-FH doses nearly 16% (p = 0.0765) lower, while the PTV doses were almost identical between the groups. Similarly, for 10 MV plans, large patients showed roughly a 23% lower bladder dose (17.16 Gy vs. 22.25 Gy; p = 0.0009) and about a 5.5% reduction in rectum dose. The PB, RT-FH, and LT-FH doses in large patients were approximately 6.6% higher, 4.7% lower, and 11.2% lower, respectively, with the PTV doses remaining comparable. Moreover, differences between 6 MV and 10 MV within each

TABLE II
The Monitor Units (MUs) Distribution for 6 MV and 10 MV Photon Energies across Small and Large Patient Groups

Patient size	6 MV MUs	10 MV MUs	p-value
Small	971±178	907±165	0.035
Large	939±199	891±235	0.141
(Small vs. Large) p-value	0.725	0.869	

http://dx.doi.org/10.14500/aro.12243

TABLE III
HOMOGENEITY INDEX (HI) AND CONFORMITY INDEX (CI): COMPARISON OF 6 MV VERSUS 10 MV PHOTON ENERGIES AND SMALL VERSUS LARGE PATIENT GROUPS

Patient size	HI			CI		
	6 MV	10 MV	p-value	6 MV	10 MV	p-value
Small	0.141±0.051	0.133±0.054	0.328	0.972±0.012	0.975±0.014	0.293
Large	0.134±0.058	0.13±0.062	0.527	0.975±0.017	0.977±0.014	0.342
(Small vs. Large) p-value	0.798	0.921		0.672	0.672	

TABLE IV
COMPARISON OF MEAN DOSE (GY) FOR THE PTV AND OARS: EFFECTS OF PHOTON ENERGY AND PATIENT SIZE

Photon energy	Patient size	Organs					
		Bladder	Rectum	PB	RT-FH	LT-FH	PTV
6 MV	Small	22.38±3.15	28.92±4.16	18.69±6.11	15.07±3.76	15.22±4.09	61.35±0.98
	Large	17.62±2.76	28.31±3.62	19.93±7.43	13.54±1.6	12.73±1.61	61.35±0.58
	p-value	0.0024	0.7336	0.7027	0.2288	0.0765	0.989
10 MV	Small	22.25±3.43	29.34±3.78	18.94±7.82	14.61±3.61	15.14±4.04	61.48±0.96
	Large	17.16±2.29	27.73±3.18	20.18±7.31	13.93±1.95	13.45±2.01	61.33±0.63
	p-value	0.0009	0.3177	0.7242	0.5949	0.2333	0.6879
p-value	Small	0.7351	0.4618	0.8517	0.2112	0.8762	0.332
(6 MV vs. 10 MV)	Large	0.116	0.1122	0.3339	0.4587	0.12	0.884

PTV: Planning target volume, PB: Penile bulb, RT-FH: Right femoral heads, LT-FH: Left femoral heads

patient group were minimal (percentage variations under 3% for all structures) and not statistically significant (p-values ranging from 0.116 to 0.884).

D. DVH Comparison

Fig. 2 displays the DVH curves for the PTV in prostate cancer IMRT plans. The curves compare 6 MV (solid lines) and 10 MV (dashed lines) plans for small (blue) and large (red) patients. In all groups, nearly 100% of the PTV receives doses of 40–55 Gy, reflecting excellent target coverage. At doses above 55 Gy, the curves gradually decline, indicating the high-dose region of the target. Notably, while both photon energies produce comparable PTV coverage, there is a subtle improvement in dose homogeneity with 10 MV plans, especially in small patients, where, for example, at 60 Gy, the volume receiving the dose is slightly higher with 10 MV compared to 6 MV. Large patients exhibit a similar pattern with nearly equivalent values.

Fig. 3 illustrates the DVH curves for OARs. The curves reveal that 10 MV plans tend to provide a modest reduction in the volume of normal tissues receiving intermediate to high doses compared to 6 MV plans. In particular, the bladder DVHs show that large patients experience a significant reduction in dose volumes compared to small patients; for example, the volume of the bladder receiving a given dose is considerably lower in large patients. The DVHs for the femoral heads exhibit similar trends, whereas the differences for the rectum and PB are smaller between photon energies and patient sizes. Those effects can be more clearly seen in the quantitative analysis of DVHs.

Table V provides quantitative DVH values for the PTV and OARs, comparing 6 MV and 10 MV photon energies in small and large patients. The PTV is uniformly well covered, with nearly 100% of the volume receiving doses between 40

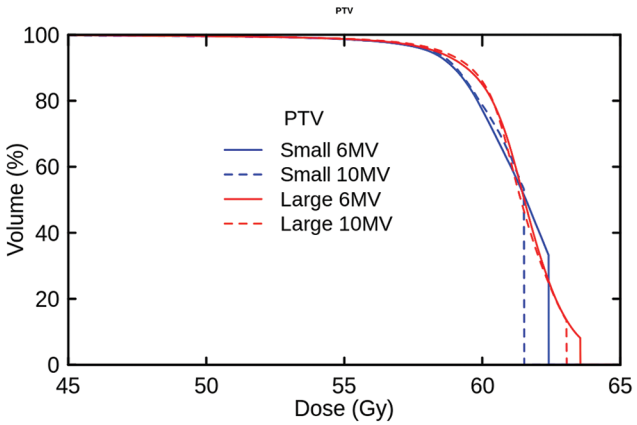

Fig. 2. Dose-volume histograms for the planning target volume: Comparison of 6 MV (solid lines) and 10 MV (dashed lines) photon energies in small (blue) and large (red) patient groups.

and 55 Gy and only minor differences at higher dose levels. For the bladder, large patients had dose volumes that were approximately 23–26% lower than those in small patients at 10 Gy ($p = 0.0035$ for 6 MV and $p = 0.0009$ for 10 MV), with similar significant reductions observed at higher doses, up to 30.3% for 6 MV and 30.9% for 10 MV at 50 Gy.

The rectum exhibited only small, non-significant differences between the groups, while the PB showed a slight increase in dose for large patients that was not statistically significant. For the femoral heads, both the right and left structures experienced notable dose reductions in large patients. In detail, the left femoral head showed a reduction of about 33.3% at 20 Gy with 6 MV and 37.3% with 10 MV, and up to 78.8% for 6 MV and 52.7% for 10 MV at 25 Gy, and as much as 96% for 6 MV and 81% for 10 MV at 30 Gy; the reduction for the left femoral head in 6 MV

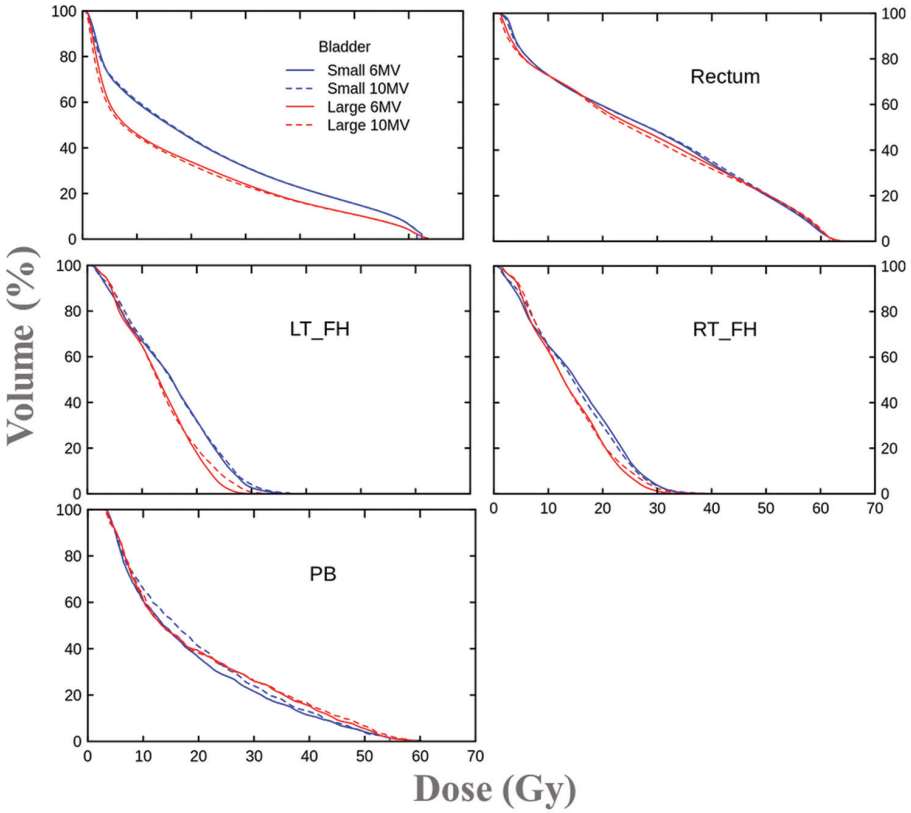

Fig. 3. Dose-volume histograms for organs at risk between 6 MV solid lines and 10 MV dashed lines among small blue and large red patient groups.

Table V
Dose Volume Histogram (DVH) Analysis for PTV and OARs

Organs	Dose	Small			Large			(Small vs. Large) p-value	
		% V 6 MV	% V 10 MV	p-value	% V 6 MV	% V 10 MV	p-value	6 MV	10 MV
PTV	55	98.4±0.9	98.4±1	0.7758	98.5±1.4	98.6±1.3	0.3164	0.8984	0.6927
	58	92.8±3	93.4±4.4	0.5036	94.2±3.2	94.8±2.6	0.2032	0.3353	0.3853
	60	67.4±27.2	70.5±24.9	0.3287	75.7±12.1	74.9±11.2	0.7452	0.3672	0.6059
	63	11.7±9.8	10±8.2	0.2994	7.5±6.6	7.3±7	0.7523	0.2666	0.4305
Bladder	10	59.7±10.7	60.5±10.8	0.3932	45.8±7.7	44.9±6.6	0.2886	0.0035	0.0009
	20	43.7±6.6	44±6	0.7001	33.7±6.6	32.3±5.3	0.1516	0.0044	0.0003
	30	31.3±4.7	31.4±4.5	0.8293	23.9±5.6	23±4.9	0.1923	0.0081	0.0016
	40	22.3±3.5	22.3±3.5	0.9585	16.1±3.8	15.9±3.2	0.6768	0.0024	0.0007
	50	15.2±2.4	15.2±2.6	0.9909	10.6±2.6	10.5±2.1	0.9160	0.0011	0.0003
Rectum	10	72.7±12.5	72.8±12.5	0.953	72.7±16.9	72.5±16.9	0.5504	0.9891	0.9714
	20	59.2±11.5	59.1±12	0.8769	57.6±9.3	56.4±8.6	0.2265	0.7375	0.5692
	30	47.7±10.2	47.9±11.5	0.8207	45.3±6.7	43.4±3.8	0.1814	0.5308	0.2293
	40	33.5±5.1	34.6±7.8	0.4357	32.6±4.4	31.3±3	0.1568	0.694	0.2145
	50	19.5±2.2	20.1±2	0.2986	20.1±2.8	20±3	0.8631	0.5976	0.8959
PB	10	60.3±21.3	65.5±22.4	0.0646	60.7±26.7	63.2±22.5	0.2637	0.9747	0.826
	20	35.9±16.4	40.6±17.2	0.0973	38.7±19.6	37.9±18.6	0.3614	0.7394	0.7431
	30	21.3±13.2	23.7±14.1	0.1814	25.8±15.6	25.7±15.1	0.8276	0.5082	0.7618
	40	11±10.2	12.5±10.5	0.1376	14.8±10.7	15.4±11.6	0.6490	0.4411	0.5883
	50	3.8±6.2	3.4±4.6	0.5573	5.1±6.7	6.2±7.2	0.5244	0.6689	0.3519
RT-FH	10	64.8±21.6	65±19.4	0.9473	62.3±15.8	63.6±13.3	0.4715	0.7679	0.8559
	20	32.1±16.7	29.2±14.3	0.1161	21.4±11.9	21.1±12.6	0.9548	0.1104	0.2037
	25	13.5±11.1	12.4±10	0.5813	7.1±7.1	9.6±9.9	0.1769	0.1353	0.5483
	30	3.4±4.2	3.2±4.9	0.7919	1.1±2.5	2.2±3.8	0.1577	0.1335	0.6073
LT-FH	10	66.6±21.4	67.8±20.2	0.2861	64.3±19.7	64.6±16.7	0.8954	0.8075	0.7065
	20	31.3±17.8	31.1±19	0.8866	17.1±11	19.4±13.3	0.5295	0.0401	0.1249
	25	13.2±13.2	14.8±14.3	0.5122	2.8±3.1	7±6.8	0.053	0.0209	0.1221
	30	2.4±3.2	3.7±5.7	0.2501	0.1±0.1	0.7±1	0.1218	0.0264	0.094

PTV: Planning target volume, PB: Penile bulb, RT-FH: Right femoral heads, LT-FH: Left femoral heads

plans reached statistical significance ($p < 0.05$) above 10 Gy. Analogs percentage reductions occurred in the right femoral head, but statistical significance remained unattainable.

The impact of switching from 6 MV to 10 MV on PTV coverage and OAR sparing was marginal and did not reach statistical significance in either size cohort. In small patients, V55 remained essentially unchanged, and V58 rose by <1%. Large patients showed similar stability, with V55 increasing by only about 0.1% and V60 actually decreasing by around 1%.

OAR sparing exhibited equally subtle but size-dependent differences. In the bladder, small patients saw a slight 1% increase in the volume receiving low doses when using 10 MV, whereas large patients experienced a modest 2% reduction. Rectal dose volumes shifted by under 1% in both groups – small-patient rectal exposure stayed virtually the same, and large-patient exposure fell only marginally. The PB followed this size-dependent pattern as well: small patients had an approximately 8% increase in volume exposed to low doses with 10 MV, while large patients saw about a 4% rise. For the right femoral head, small patients benefited from 10 MV with about 7% less volume receiving higher doses (25–30 Gy). In large patients, however, 10 MV increased those same volumes by about 35%. Conversely, the left femoral head was consistently better spared by 6 MV in both cohorts: small patients had approximately 12% less volume above 25 Gy with 6 MV, and large patients enjoyed an even greater advantage of about 60% less volume at that same threshold.

IV. Discussion

The research examined how photon energy (6 MV vs. 10 MV) and patient size affected IMRT plans for prostate cancer treatment by showing mutual effects on treatment quality. To the best of our knowledge, this is the first study to compare the effects of photon energy under a moderate hypofractionation protocol delivering a PTV dose of 60.0 Gy in 20 fractions (3 Gy per fraction), to statistically analyze the effect of photon energy in localized prostate IMRT planning, and to assess the influence of patient size on IMRT planning.

The target coverage remained excellent with similar results between both energies, but differences emerged in MUs requirements and normal tissue sparing, which patient size helped to shape.

For each photon energy, patient size had a measurable impact on dose distributions. The 10 MV treatment plans performed on small patients demonstrated better treatment efficiency through significant MU reduction, as the plans needed 6.6% fewer MUs compared to 6 MV plans. Conversely, although large patients also exhibited a reduction in MUs with 10 MV, the difference did not reach statistical significance, indicating that the energy-related benefits on MU reduction might be more pronounced in smaller patients. Higher MUs increase leakage radiation, which is expected to raise the risk of secondary malignancies and affect blood parameters (Mohammed, Ismail and Tahir, 2025).

The effect of patient size was even more evident when evaluating normal tissue doses. Large patients had approximately 21% (6 MV) and 23% (10 MV) lower mean bladder doses compared to small patients. Similarly, Bladder V10 values were reduced by 23–26% in large patients, regardless of photon energy. This relationship between larger patient size and reduced doses remained consistent all the way from V10 through V50, suggesting a natural decrease in dose distribution with increasing body size. The impact on the left femoral head was even more striking: with 6 MV plans, large patients exhibited about a 33.3% reduction at 20 Gy, up to 78.8% at 25 Gy, and as much as 96% at 30 Gy relative to small patients.

It is hard to determine a direct comparison between our results on patient-size effects and the publication scarcity on localized prostate cancer IMRT planning. Stanley, et al., in 2015 examined the linear relationship between 6 MV and 10 MV dose differences and patient size in VMAT plans, but they did not evaluate the relationship of individual photon energies with patient size. They reported a linear relationship between patient APD and relative difference in PTV R50 (the volume of PTV receiving at least 50% of the prescription dose per total PTV volume) between the 6MV and 10MV (in favor of 10MV), but their VMAT technique is not directly comparable with our IMRT procedure.

Interestingly, our results are opposite to this known effect of the breast size in breast cancer radiotherapy, whereby smaller breast sizes attain better OAR sparing. This implies that the effects of patient size are dependent on the tumor site.

Thanks to Solaiappan, et al., in 2009, who reported raw bladder and rectum dose data alongside patient APD and LRD measurements, we were able to perform a statistical reanalysis and compare their outcomes with ours. They treated 20 localized prostate cancer patients (79.2 Gy in 44 fractions, 5 beams) with 6 MV and 10 MV IMRT but did not conduct statistical tests. Applying a similar analytic approach, we partitioned their cohort as small (n = 12) and large (n = 8) patients at a mean size of 29.63 cm. The mean dose of bladder and rectum stratified by patient size and photon energy are given in Table VI.

TABLE VI
Analysis of Mean Dose (Gy) to Bladder and Rectum from Reference (Solaiappan, et al., 2009), Comparing the Effects of Photon Energy and Patient Size

Organs	Small			Large			(Small vs. Large) p-value	
	6 MV	10 MV	p-value	6 MV	10 MV	p-value	6 MV	10 MV
Bladder	40.8±12.0	40.2±11.0	0.6301	29.0±13.2	28.3±13.8	0.613	0.0524	0.0461
Rectum	38.0±15.0	37.3±14.5	0.1657	44.9±8.1	45.0±8.5	0.9178	0.2477	0.1935

Interestingly, the results of Solaiappan, et al., in 2009 show a trend toward a significant reduction in bladder mean dose of 28.9% in large patients treated with 6 MV ($p = 0.0524$) and a significant reduction of 29.6% with 10 MV ($p = 0.0461$). This finding confirms the robustness of bladder sparing in larger patients, independent of prescription dose and beam number – factors known to influence photon-energy effects.

We have found no significant advantage to switching 6 MV to 10 MV in either PTV coverage or OAR sparing – except that there is an advantage of reduced MUs in small patients using 10 MV. Moreover, photon energy has a subtle effect dependent on the size of the patient, and without specific statistical analysis and size-based sampling, studies run the risk of engaging in conflicting findings.

Our results in relation to lower MU obtained with 10 MV in small patients compared to Chung, et al., 2011 (PTV dose = 66 Gy) confirm our inference, but their 13% MU reduction with 15 MV is higher than our finding, probably because they compared higher photon energies. Conversely, their result of marginal bladder and rectum sparing differs from our observations in small patients, yet matches our large-patient cohort. A similar size-dependent reversal appears (Solaiappan, et al., 2009) (Table VI) for the rectum: when we re-analyzed their metrics without size stratification, we still observed only marginal, non-significant differences. Beyond the absence of statistical testing in earlier studies, differences in dose calculation algorithms (Agid and Hassan, 2025) and the number of beams may also explain the discrepancies. Pirzkall, et al., in 2002 demonstrated that photon-energy effects disappear when equal to or more than nine beams are used in prostate IMRT planning.

Finally, our results do not coincide with the results of Sung, et al., in 2012 in prostate cases with the seminal vesicles, finding that with increased energies, rectal-wall and femoral-head doses were reduced significantly. This implies that the effects of photon-energy might be tumor-stage dependent.

Overall, the results indicate normal-tissue protection depends most heavily on patient size rather than on higher-energy photon beams. Future clinical trials need to adopt patient-specific anatomical metrics to provide truly personalized treatment while reducing toxicity. The retrospective approach of this study, together with its smaller cohort, represents important limitations that must be addressed by future research using prospective methods with expanded participant numbers.

V. Conclusion

This study set out to determine how photon-energy selection (6 MV vs. 10 MV) and patient anatomical size influence IMRT plan quality in localized prostate cancer. Our results confirm that both 6 MV and 10 MV beams deliver equally excellent PTV coverage, with only a modest 6.6% reduction in MUs observed in small patients when moving to 10 MV. Changes in OAR doses due to photon energy alone were minimal and varied with patient size. By contrast, patient size exerted a profound effect: large patients experienced 21–23% lower mean bladder doses and 23–30% reductions in bladder V10–V50, regardless of beam energy, and showed 33–96% decreases in left femoral-head V20–V30 (significant for 6 MV). These findings demonstrate that patient size–not photon energy–is the dominant determinant of normal-tissue sparing. Accordingly, future energy-comparison studies, treatment-planning protocols, and clinical trials must stratify or adjust for patient anatomy to achieve truly individualized, toxicity-minimizing IMRT.

VI. Acknowledgments

The authors express sincere gratitude to Zhianawa Cancer Center in Sulaimani, Iraq, for providing access to patient data and supporting this research project. We extend our deep appreciation to the medical physics team, particularly Hunar Hassan and Zarean Saeed, and to the oncology team, specifically Sazgar Majeed and Nyan Saeed, for their essential contributions to treatment planning and data collection.

References

Agid, R.S., and Hassan, F.F., 2025. Evaluation of 3D-CRT treatment planning techniques for breast cancer: A comparative study of collapsed cone and Monte Carlo algorithms using new quality indices. *ARO-The Scientific Journal of Koya University*, 13(2), pp.134-141.

Agrawal, R., Dey, A., Datta, S., Nassar, A., Grubb, W., Traughber, B., Biswas, T., Ove, R., and Podder, T., 2022. Pattern of radiotherapy treatment in low-risk, intermediate-risk, and high-risk prostate cancer patients: Analysis of national cancer database. *Cancers*, 14(22), p.5503.

Bergengren, O., Pekala, K.R., Matsoukas, K., Fainberg, J., Mungovan, S.F., Bratt, O., Bray, F., Brawley, O., Luckenbaugh, A.N., Mucci, L., Morgan, T.M., and Carlsson, S.V., 2023. 2022 update on prostate cancer epidemiology and risk factors-a systematic review. *European Urology*, 84(2), pp.191-206.

Bhatnagar, A.K., Heron, D.E., Deutsch, M., Brandner, E., Wu, A. and Kalnicki, S., 2006. Does breast size affect the scatter dose to the ipsilateral lung, heart, or contralateral breast in primary breast irradiation using intensity-modulated radiation therapy (IMRT)? *American Journal of Clinical Oncology*, 29(1), pp.80-84.

Boone, J., Strauss, K.J., and Cody, D.D., 2011. *Size-Specific Dose Estimates (SSDE) in Pediatric and Adult Body CT Examinations*. AAPM, Washington, DC.

Chung, J.B., Kim, J.S., Kim, I.A., Lee, J.W., Cho, W., and Suh, T.S., 2011. The effect of photon energy on the intensity-modulated radiation therapy plan for prostate cancer: A planning study. *Journal of the Korean Physical Society*, 59(1), pp.183-188.

De Boer, S.F., Kumek, Y., Jaggernauth, W. and Podgorsak, M.B., 2007. The effect of beam energy on the quality of IMRT plans for prostate conformal radiotherapy. *Technology in Cancer Research and Treatment*, 6(2), pp.139-146.

Dearnaley, D., Syndikus, I., Mossop, H., Khoo, V., Birtle, A., Bloomfield, D., Graham, J., Kirkbride, P., Logue, J., Malik, Z., Money-Kyrle, J., O'Sullivan, J.M., Panades, M., Parker, C., Patterson, H., Scrase, C., Staffurth, J., Stockdale, A., Tremlett, J., Bidmead, M., Mayles, H., Naismith, O., South, C., Gao, A., Cruickshank, C., Hassan, S., Pugh, J., Griffin, C., Hall, E., and CHHiP Investigators., 2016. Conventional versus hypofractionated high-dose intensity-modulated radiotherapy for prostate cancer: 5-year outcomes of the randomised, non-inferiority, phase 3 CHHiP trial. *The Lancet Oncology*, 17(8), pp.1047-1060.

Evans, A.J., 2018. Treatment effects in prostate cancer. *Modern Pathology*, 31, pp.110-121.

Followill, D.S., Nüsslin, F., and Orton, C.G., 2007. IMRT should not be administered at photon energies greater than. *Medical Physics*, 34(6Part1), pp.1877-1879.

Hatano, K., Tohyama, N., Kodama, T., Okabe, N., Sakai, M., and Konoeda, K., 2019. Current status of intensity-modulated radiation therapy for prostate cancer: History, clinical results and future directions. *International Journal of Urology*, 26(8), pp.775-784.

ICRU., 2010. Prescribing, recording, and reporting photon-beam intensity-modulated radiation therapy (IMRT): Contents. *Journal of the ICRU*, 10(1), p.NP.3-NP.

Kry, S.F., Salehpour, M., Followill, D.S., Stovall, M., Kuban, D.A., Allen White, R., and Rosen, I.I., 2005. Out-of-field photon and neutron dose equivalents from step-and-shoot intensity-modulated radiation therapy. *International Journal of Radiation Oncology Biology Physics*, 62(4), pp.1204-1216.

Lin, J., Zhan, X., Chen, R., Chen, R., Jiang, M., Li, Y., Liu, X., Chen, G., and Fu, B., 2023. Increased burden of second bladder cancer and rectal cancer in prostate cancer treated with radiotherapy: Results from surveillance, epidemiology, and end results. *Cancer Control*, 30, p.10732748231177544.

Mohammed, B.N., Ismail, A.H., and Tahir, E.M., 2025. Assessment of leakage radiation and radiobiological impacts in gamma knife radiosurgery: Dosimetric and biological analysis. *ARO-The Scientific Journal of Koya University*, 13(1), pp.284-290.

Morgan, S.C., Hoffman, K., Andrew Loblaw, D., Buyyounouski, M.K., Patton, C., Barocas, D., Bentzen, S., Chang, M., Efstathiou, J., Greany, P., Halvorsen, P., Koontz, B.F., Lawton, C., Marc Leyrer, C., Lin, D., Ray, M., and Sandler, H., 2018. Hypofractionated radiation therapy for localized prostate cancer: An ASTRO, ASCO, and AUA evidence-based guideline. *Journal of Clinical Oncology*, 36(34), pp.3411-3430.

Mottet, N., van den Bergh, R.C.N., Briers, E., Van den Broeck, T., Cumberbatch, M.G., De Santis, M., Fanti, S., Fossati, N., Gandaglia, G., Gillessen, S., Grivas, N., Grummet, J., Henry, A.M.,… & Cornford, P., 2021. EAU-EANM-ESTRO-ESUR-SIOG guidelines on prostate cancer-2020 update. Part 1: Screening, diagnosis, and local treatment with curative intent. *European Urology*, 79(2), pp.243-262.

Mukherjee, K., Small, W. and Duszak, R., 2022, Trends and variations in utilization and costs of radiotherapy for prostate cancer: A SEER medicare analysis from 2007 through 2016. *Brachytherapy*, 21(1), pp.12-21.

Pirzkall, A., Carol, M.P., Pickett, B., Xia, P., Roach, M. 3rd., and Verhey, L.J., 2002. The effect of beam energy and number of fields on photon-based IMRT for deep-seated targets. *International Journal of Radiation Oncology Biology Physics*, 53(2), pp.434-442.

Pryor, D.I., Turner, S.L., Tai, K.H., Tang, C., Sasso, G., Dreosti, M., Woo, H.H., Wilton, L., and Martin, J.M., 2018. Moderate hypofractionation for prostate cancer: A user's guide. *Journal of Medical Imaging and Radiation Oncology*, 62(2), pp.232-239.

Ratosa, I., Jenko, A., and Oblak, I., 2018. Breast size impact on adjuvant radiotherapy adverse effects and dose parameters in treatment planning. *Radiology and Oncology*, 52(3), pp.233-244.

Raychaudhuri, R., Lin, D.W., and Montgomery, R.B., 2025. Prostate cancer: A review. *JAMA*, 33(10), pp.1433-1446.

Schafer, E.J., Laversanne, M., Sung, H., Soerjomataram, I., Briganti, A., Dahut, W., Bray, F., and Jemal, A., 2025. Recent patterns and trends in global prostate cancer incidence and mortality: An update. *European Urology*, 87(3), pp.302-313.

Sethi, A., Leo, P., Kabat, C., and Cecilio, P., 2013. SU-E-T-538: Validation of Monte Carlo Dose algorithm in heterogeneous medium. *Medical Physics*, 40(6Part19), pp.329-329.

Solaiappan, G., Singaravelu, G., Prakasarao, A., Rabbani, B., and Supe, S.S., 2009. Influence of photon beam energy on IMRT plan quality for radiotherapy of prostate cancer. *Reports of Practical Oncology and Radiotherapy*, 14(1), pp.18-31.

Stanley, D.N., Popp, T., Ha, C.S., Swanson, G.P., Eng, T.Y., Papanikolaou, N., and Gutiérrez, A.N., 2015. Dosimetric effect of photon beam energy on volumetric modulated arc therapy treatment plan quality due to body habitus in advanced prostate cancer. *Practical Radiation Oncology*, 5(6), pp.e625-e633.

Sung, W., Park, J.M., Choi, C.H., Ha, S.W., and Ye, S.J., 2012. The effect of photon energy on intensity-modulated radiation therapy (IMRT) plans for prostate cancer. *Radiation Oncology Journal*, 30(1), p.27-35.

RStudio Team (2022). *RStudio: Integrated Development Environment for R. Boston*, MA: RStudio, PBC. Available at: http://www.rstudio.com/

Teo, M.Y., Rathkopf, D.E., and Kantoff, P., 2019. Treatment of advanced prostate cancer. *Annual Review of Medicine*, 70(1), pp.479-499.

Thangavelu, S., Jayakumar, S., Govindarajan, K.N., Supe, S.S., Nagarajan, V., and Nagarajan, M., 2011. Influence of photon energy on the quality of prostate intensity modulated radiation therapy plans based on analysis of physical indices. *Journal of Medical Physics*, 36(1), pp.29-34.

Webb, S., 2003. The physical basis of IMRT and inverse planning. *The British Journal of Radiology*, 76(910), pp.678-689.

Zhai, D.Y., Yin, Y., Gong, G.Z., Liu, T.H., Chen, J.H., Ma, C.S., and Lu, J., 2013. RapidArc radiotherapy for whole pelvic lymph node in cervical cancer with 6 and 15 MV: A treatment planning comparison with fixed field IMRT. *Journal of Radiation Research*, 54(1), pp.166-173.